DOI: 10.21062/mft.2021.022 http://www.journalmt.com

Experimental Characterization of Microcomposite Magnetorheological Elastomer

Salah Rouabah[1], Salah Aguib[2], Mohamed Hadji[1], Lallia Kobzili[2]
[1]Laboratory of Studies and Research in Industrial Technology, University of Saad Dahleb Blida1, Algeria.
rouabah.salah@univ-blida.dz, hadji_n@yahoo.com
[2]Dynamic Motors and Vibroacoustic Laboratory, Faculty of Technology, University of Boumerdes35000, Algeria.
s.aguib@univ-boumerdes.dz, l.kobzili@univ-boumerdes.dz

This work presents an analysis experimental of dynamic properties of microcomposite magnetorheological elastomer (MMRE) by a dynamic mechanical analyzer (DMA). The charge of magnetized iron particles is 30% of the total volume. A dynamic mechanical analysis DMA was carried out, in the scanning mode of the amplitude of shear strain, and for magnetic field densities varying from 0mT to 325mT. The storage modulus G' and the loss modulus G", of the elastomer decrease, when the amplitude of the strain increases. This trend is more pronounced under a higher magnetic flux density (250mT and 325mT). In the presence of the magnetic field, the level of these two dynamic moduli and of the damping increases considerably, passing from one value to another of the applied external magnetic field. As a result, the MR effect of MRE elastomers has increased significantly with increasing magnetic flux density.

Keywords: Microcomposite, Magnetorheological elastomer, Magnetic flux density, Dynamic mechanical properties, Iron particles.

1 Introduction

Microcomposite magnetorheological elastomers (MMRE) belong to the family of intelligent composite materials, their rheological properties can be effectively controlled in near real time in a continuous manner and reversible by the application of an external magnetic field.

Studies from several available literatures on the preparation of MRE elastomeric composites describe that MRE composites are an elastomeric matrix, a ferromagnetic charge of micrometric size and certain additives such as crosslinking agents, antioxidants and mixing aids can be used. The experimental results demonstrate that the addition of carbon black improves the mechanical properties of the magnetorheological elastomer. The effect of temperature on the dynamic mechanical properties of MR elastomers has been examined by Wan et al. [1] The samples of anisotropic MR elastomers exposed to variable temperatures and magnetic fields were prepared. The dynamic moduli depending on the temperature and the frequency of the MRE samples were modeled. In the study carried out by Dargahi et al. [2], the static and dynamic properties of different types of MR elastomers were studied, under a shear strain amplitude ranging from 2.5 to 20%, in the range of frequencies 0.1–50 Hz, and a variable magnetic flux density (0mT–450mT). The effect of the nature of the particles on the mechanical properties and the magnetic effect of elastomers MRE have been studied by Kumar et al. [3] According to this study, the use of RTV silicone rubber, charged with hybrid MRE based on carbon nanomaterials, improved the compression modulus and therefore the mechanical properties. Rui et al. [4] realized a numerical analysis on domed magnetorheological elastomers for sheet metal. The velocity and stress distribution of the sheet metal under different magnetic intensities are compared and analyzed. The results show that the shear modulus of the magnetorheological elastomer increases with the increase of the magnetic intensities, and the configuration changes from elliptical to the conical shape. The rheological properties of a new magnetorheological elastomer (MRE) charged with plate-shaped carbonyl iron magnetic particles (CIP) were investigated by Hapipi et al. [5] Plate-shaped (MRE-P) and spherical (MRE-S) MRE samples were prepared. It was observed that, the MRE-P elastomer demonstrated a higher storage modulus and a lower loss factor than MRE-S. The MR effect of MRE-P is slightly lower than that of MRE-S (114% and 137%) In addition, and by a study carried out by Zhang et al. [6], the dynamic rheological behavior of magnetorheological gels, with different weight fractions of CIP particles suspended in polyurethane (PU) was examined. The microstructural variation of the chains of self-assembled copolymer and magnetically induced CIP chains at different strain amplitudes, applied coil intensities, and CIP weight

fractions is offered as an explanation of the nonlinear rheological behaviors of PU-based MR gels. Nam et al. [7] presented experimental research and numerical modeling of the dynamic properties of magnetorheological elastomers (MRE). More recently, Vatandoost et al. [8], experimentally examined the dynamic properties of isotropic and anisotropic MRE in the compression mode, under wide ranges of strain amplitude (2.5-20%), excitation frequency (0.1–50 Hz) and magnetic flux density (0mT–750mT), superimposed on a large static pre-strain (21%). Large changes in the storage modulus and the loss factor in compression mode have been observed. So better MR effects. Agirre-Olabide et al. [9] have developed a new technique of magneto-dynamic compression to measure the magnetoiscoelastic properties of magnetorheological elastomers (MRE) at high frequencies. Isotropic MREs filled with carbonyl iron powder were synthesised, and three volumetric particle contents were studied 0%, 15% and 30%. The dynamic properties of isotropic and anisotropic MREs were determined by the use of a double overlap shear test under harmonic loading in the displacement control mode. Effects of excitation frequency, strain amplitude, and magnetic field intensity on the dynamic properties of the MREs were examined.Michal et al. [10] have developed a composite material based on a geopolymer matrix and a reinforcement of basalt fibers. Research on the reinforcement of geopolymer material with layers of basalt fabrics was carried out in order to verify the improvement of mechanical properties in relation to non-reinforced material. Bodnaruk et al. [11] have shown that the "constant" magnetic anisotropy is a consequence of particles displacements and a characteristic of the energy of internal deformations in the polymer matrix. The maximum anisotropy constant of the filling is at least one order of magnitude larger than the shear modulus of the pure elastomer (matrix). In a magnetic field, the gain in the rigidity of the composite material is attributed to the magnetomechanical coupling, which is in turn a source of anisotropy. Agirre-Olabide et al. [12] have developed a new magneto-viscoelastic model for anisotropic magnetorheological elastomers (MREs), which combines the dynamic behavior and magnetic permeability components. Five samples were synthesised with different particle contents. Dynamic properties were measured using a rheometer equipped with a magnetorheological cell. Zuzana et al. [13] Have studied the effects of the reinforcement phase in particulate ceramic composites on their properties.The microstructure, density, hardness and fracture toughness of Si_3N_4 + SiC ceramic composite materials were compared with monolithic Si_3N_4 based ceramic material. Drahomír et al. [14] Have prepared a composite material of magnesium by extrusion of chemically treated powders. Microstructures with partially preserved borders between particles containing specific elements depending on the preparation method were created by extrusion.

Vibrations being considered as one of the worst problems in various sectors: aeronautics, automobiles, Building, ext. In the currents scientific world, several techniques and methods of attenuation and vibration Control are used to protect infrastructure, my last remains always limited in time. In this context, the aim of this Work is to use smart magnetorheological elastomer to continuously monitor vibrations in real time.

2 Analytical modeling

To describe the behavior of the magnetorheological elastomer composite, a micromechanical analytical model has been developed on an elementary cell which can generate a representative chain by replication along the axis of the chain. This cell is a cylinder, a real agglomerate of the composite; it consists of two hemispheres coated in a large cylinder of elastomer. The application of adequate boundary conditions (described below) on the surface of this cylinder builds a chain structure in the direction of loading. In reality, the magnetorheological composite has a very complex microstructure; one can think of aggregates disturbing the arrangement of chains, misalignment and length of chains. Figure 1 was performed with an optical microscope. There are columnar aggregates formed of several particle thicknesses. The finest area could be observed by electron microscope and the area separating the particles increases.

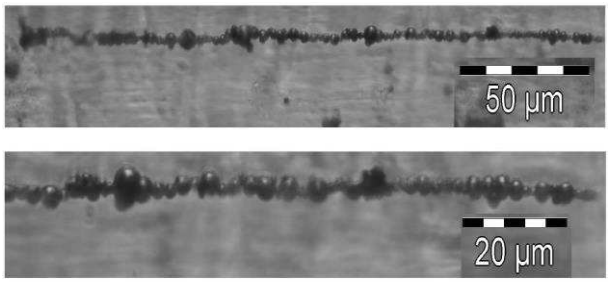

Fig. 1 *Section of the structured composite observed by optical microscope.*

The approach adopted is to isolate the important physical parameters for this type of system, namely: the anisotropic structure, the gap separating two particles within the same chain, and the volume fraction of the charges. The overall structure is thus seen as made of particles ideally spaced by the same gap g, making the ratio of the gap over the radius g/a of the particles the essential parameter of this model. The volume fraction ϕ fixes the inter-chain distance, represented here by the quantity L. L is the thickness of the elastomer ring surrounding the particles, and is

calculated as a function of the ratio g/a and of the volume fraction ϕ of inclusions, given as follows:

$$\phi = \frac{V_{Particles}}{V_{Matrix}+V_{Particles}} \quad (1)$$

The experimental investigation was realized to determine the dynamic properties of the MRE over the strain amplitude, magnetic flux density. The MRE samples are subjected to harmonic loading with static pre-displacement u_0=0.5 mm. The loss factor was determined by:

$$\tan\delta = \frac{G''}{G'} \quad (2)$$

Where:

$$G' = G^* \cos(\delta) \quad (3)$$

$$G'' = G^* \sin(\delta) \quad (4)$$

The complex modulus (G*) is the ratio of the shear stress τ(t) and shear strain γ(t), given as follows:

$$\phi = \frac{\tau_a}{\gamma_a} \quad (5)$$

The energy dissipation D per loading cycle is given as:

$$D = \int_0^T \tau(t)\dot{\gamma}(t)dt = \pi\gamma_a^2 G^* \sin(\delta) = \pi\gamma_a^2 G'' \quad (6)$$

3 Experimental analysis

The aim of this study consists in determining the magneto mechanical characteristics with a loading rate of 30% of iron particles; where the oscillation frequency is fixed at 50Hz.

3.1 Elaboration of microcomposite magnetorheological elastomer

The elastomer is prepared by the following steps:

We put a mixture of silicone oil and RTV141A polymer in a vessel and conduct a manual mixing for 10 minutes to obtain a gel elastomer with good homogenization. A second container containing a quantity of iron particles of micrometric size for charging the elastomer is provided. An amount of the obtained gel formed of silicone and RTV141A is mixed for 15 minutes with a quantity of iron particles until a homogeneous paw. By this method, an elastomer charged with 30% of iron particles was prepared. We degassed the lug obtained in vacuum for 10 minutes to remove air bubbles infiltrated during mixing, to obtain a sain structure in the experimentation. The elastomer obtained is hermetically stored at low temperature. These steps are illustrated in Figure 2. Table1 represents the ingredients in masse of the elaborated elastomer. The characteristics of the ferromagnetic particles are given by the table 2 and the characteristics of the elastomer (RTV141) are given by the Table 1. Experimental data are given in appendix A.

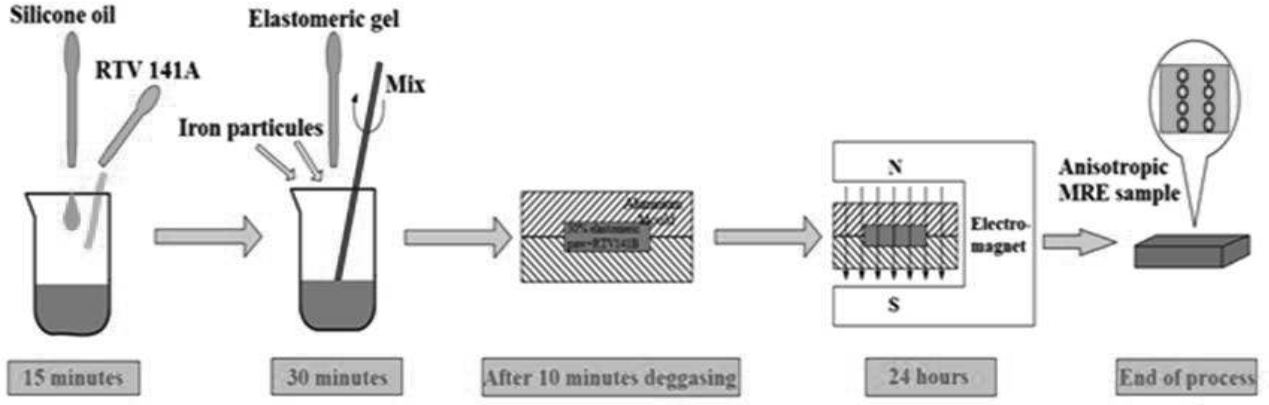

Fig. 2 *Steps of microcomposite magnetorheological elastomer elaboration.*

Tab. 1 *MMRE ingredients in mass loaded to 30% of ferromagnetic particles [15]*

Crosslinking time in hours	$m_{silicone\ oil}$ (g)	$m_{RTV(A)}$ (g)	m_{Fe} (g)	$m_{RTV(B)}$ (g)
20h30	1.064	1.0385	7.559	0.104

4 Results and discussions

The average moduli dynamic strain curves Figures 3a-d and 4a-d represent the response of the microcomposite magnetorheological elastomer subjected to a dynamic strain scanning. The storage modulus G' and the loss modulus G" are presented according to the strain amplitude, with a constant frequency of 50Hz and under a constant magnetic flux density at several values of 0mT, 100mT, 250mT and 325mT. These dynamic moduli are considered as key parameters to determine the rheological properties of microcomposite magnetorheological elastomer.

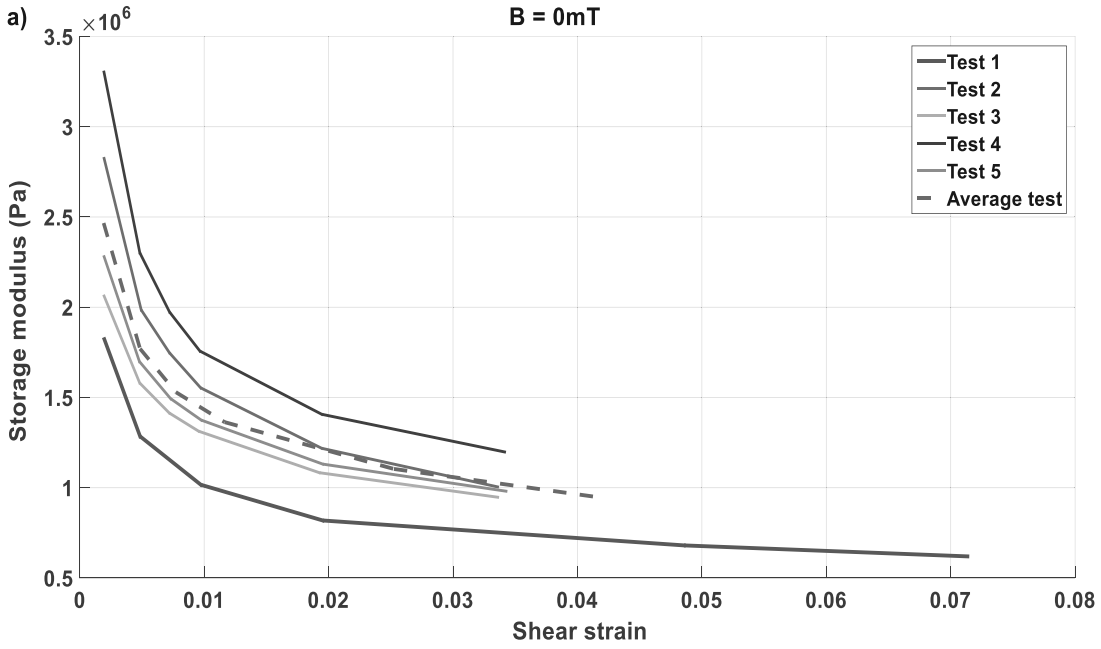
a)
B = 0mT
×10^6
Storage modulus (Pa)
Shear strain
Test 1
Test 2
Test 3
Test 4
Test 5
Average test

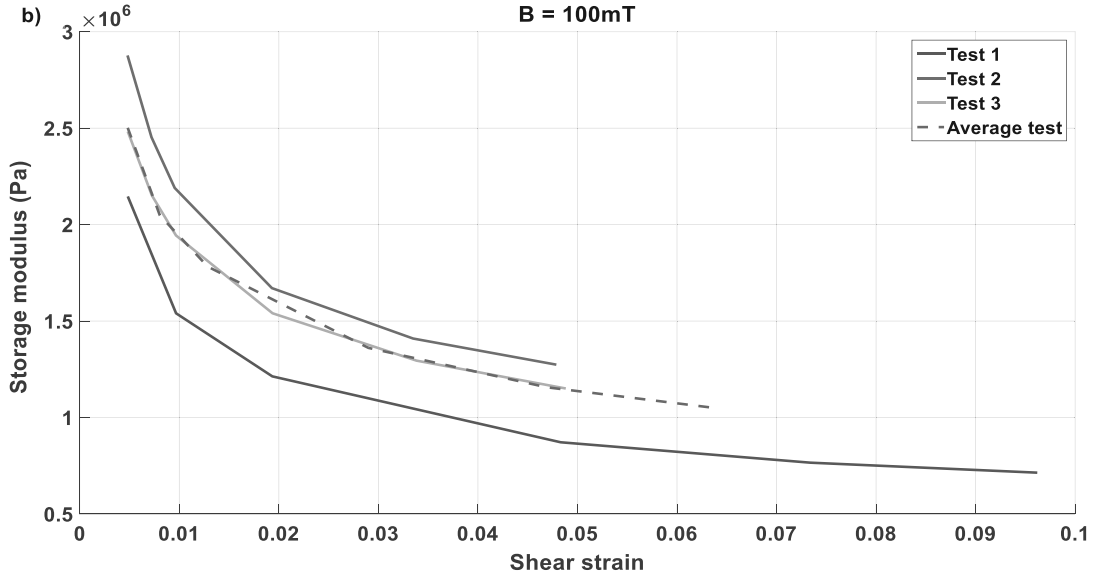
b)
B = 100mT
×10^6
Storage modulus (Pa)
Shear strain
Test 1
Test 2
Test 3
Average test

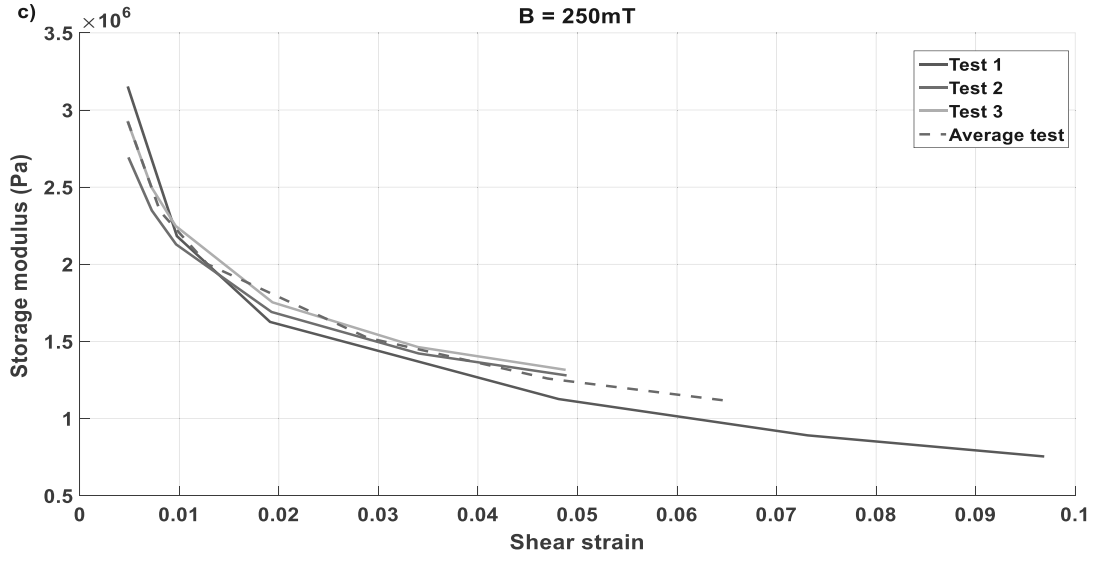
c)
B = 250mT
×10^6
Storage modulus (Pa)
Shear strain
Test 1
Test 2
Test 3
Average test

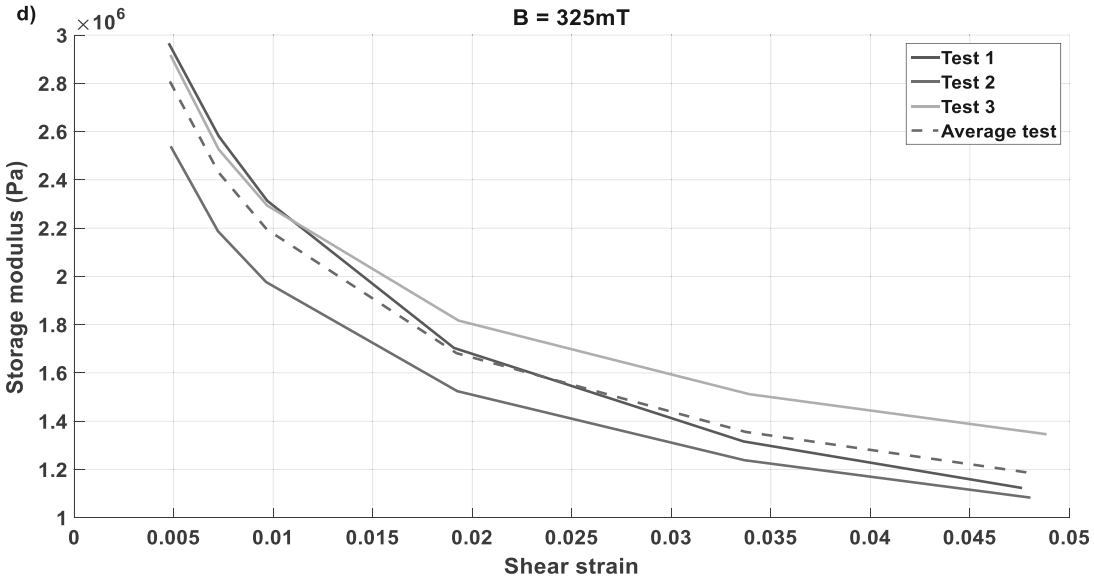

Fig. 3 *Average storage modulus as a function of different magnetic field intensities.*

At zero magnetic field, the microcomposite magnetorheological elastomer has lower storage and loss moduli. The values of these two moduli become higher when the magnetic field increases, this phenomenon is induced by the MR effect of the elastomer. In addition, the shear damping factor δ is the measure of the damping performance of the elastomer, it is defined as the ratio of the energy dissipated by damping to the stored elastic energy. The Figures (3a-d, 4a-d) show the dependence in strain amplitude of the storage and loss moduli for a given magnetic flux. These figures clearly show that the two moduli G' and G" decrease with increasing strain amplitude. The rate of decrease of these two moduli is appreciably rapid at low strain amplitudes up to 3%, while this decrease becomes slower for high strain amplitudes. This considerable change in these two moduli, with the increase in the strain amplitude, reflects the non-linearity induced by the strain.

Physically, the increase in the strain shear amplitude leads to changes in the microstructure of the MRE; the deformation of the polymer matrix increases, and the sliding between the CIP magnetic particles and the matrix increases, which will cause the rupture between the bonds connecting the polymer network and the CIP. This leads to a decrease in the dynamic moduli G' and G" of the MRE and the microstructure formed by the destroyed particles.

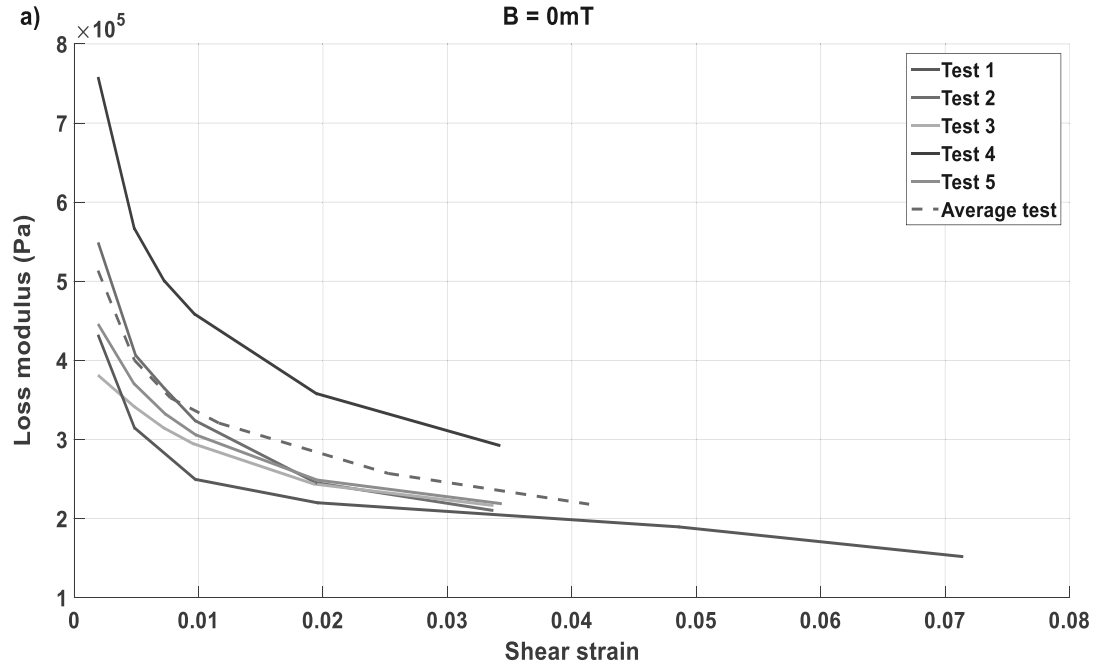

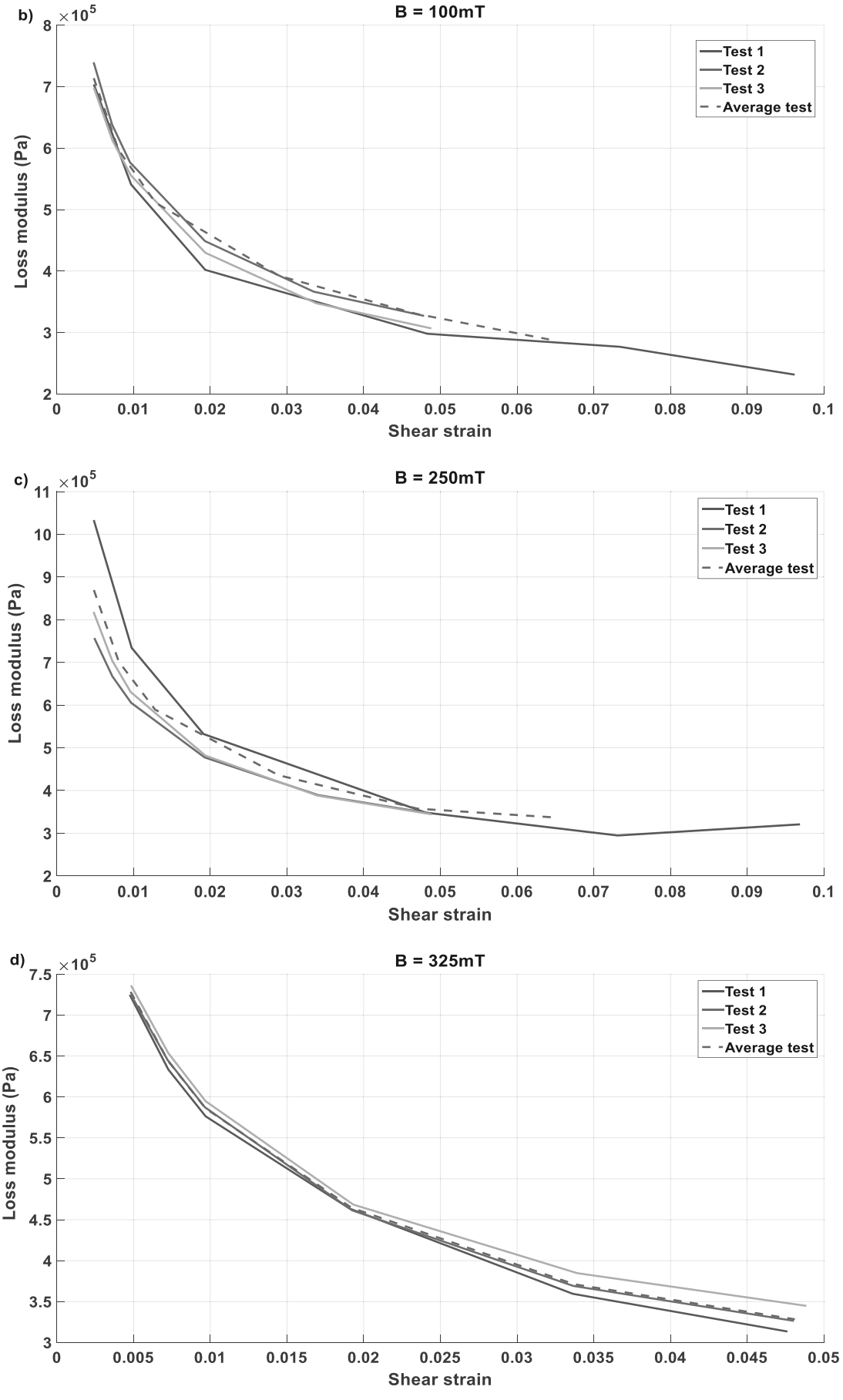

Fig. 4 *Average loss modulus according to different magnetic field intensities.*

The effect of the applied external magnetic field, on the storage modulus G' and loss modulus G", of the MRE in shear is notably more observed, in particular under a high magnetic flux density (250mT and 325mT). In the presence of the magnetic field, the values of G' and G" increased considerably (Fig. 3a,b and 4a,b), and then this increase became less important, passing from one value to another of the applied magnetic field.

In terms of value, the storage modulus G' is higher than the loss modulus G", the elastic component is dominant to that viscous, the MRE material presents a behavior of solid type.In addition, the loss modulus G" is more sensitive to the presence of the magnetic field, than the storage modulus G'. The increase in G" is greater (Figs. 3b, 4b), compared to that of G' (Fig. 3b,c,d), passing from the case without magnetic field (0mT) to the case with magnetic field (100mT, 250mT and 325mT). It is useful to note that the viscoelastic region of the MRE, not shown here, is linear (LVE). The corresponding value of the equivalent strain amplitude can be considered between 0–0.10%. In our case, the oscillatory shear test recorded the data for an amplitude of 0.5%.

5 Conclusion

In this work, an experimental study of the dynamic properties of microcomposite magnetorheological elastomer (MMRE) was carried out, under the scanning mode of the amplitude of shear strain, and for a range of densities of applied magnetic field (0mT, 100mT, 250mT and 325mT). The dynamic properties of the MMRE with a volume fraction of 30% of the magnetic particles have shown a behavior of solid typeof magnetorheological elastomers. From the results of the experiments in this article, the following conclusions can be drawn:

Physically, the decrease in the storage and loss moduli, due to the increased of shear strain, can be explained by the strain of the polymer matrix and the slip between the magnetic particles and the MRE matrix. The effect of the external applied magnetic field, on the storage and loss moduli, of the MRE elastomer in shear is highlighted. A significant increase in the storage modulus is observed, in the presence of the magnetic field, in particular under a high magnetic flux density (250mT and 325mT).

An opportunity to develop new intelligent materials based on MRE elastomers, intended to fulfill a function in a system or to serve a well-defined industrial application is offered, by means of mastering the characteristic responses, as well as the dynamic behavior, influenced by numerous parameters such as the intensity of the magnetic field, the amplitude of the deformation, as well as the nature, composition, arrangement of component elements and the volume fraction of charge particles. These parameters will allow the desired rheological properties of these materials to be controlled in advance. Of literature [16], these smart materials (The magnetorheological fluid and magnetorheological elastomer), are of great interest in realizing damping variability or stiffness variability for vibration control and mechanical shock remediation in a wide range of civil (buildings) and mechanical structures (automotive). Magnetorheological fluids (FMR) have the property of variable damping and Magnetorheological elastomer (MRE) changes their stiffness in milliseconds in the presence of a magnetic field.

Acknowledgement

The authors would like to warmly thank the mechanical behavior of materials research team for the scientific assistance provided, Dynamics of motors and vibroacoustics laboratory - University of Boumerdes.

References

[1] WAN, Y., XIONG, Y., ZHANG, S. (2018). Temperature dependent dynamic mechanical properties of Magnetorheological elastomers: Experiment and modeling. In: *Composite Structures,* Vol. 202, No., pp. 768–773.

[2] DARGAHI, A., SEDAGHATI, R., RAKHEJA, S. (2019). On the properties of magnetorheological elastomer in shear mode: Design, fabrication and characterization. In: *Composites Part B,* Vol. 159, No., pp. 269–283.

[3] KUMAR, V., LEE D-J. (2019). Mechanical properties and magnetic effect of new magneto-rheological elastomers filled with multiwall carbon nanotubes and iron particles. In: *Journal of Magnetism and Magnetic Materials,* Vol. 482, No., pp. 329–335.

[4] RUI, Z., CHAO, Y., XIAO, L., ZHONG-JIN W. (2020). The numerical analysis of the magnetorheological elastomer bulging for sheet metal. In: *Procedia Manufacturing,* Vol. 50, No., pp. 110–113.

[5] HAPIPI, N., AISHAH, S., AZIZ, A., SAIFUL, A. M., UBAIDILLAH, SEUNG B. C., NORZILAWATI, M., MUNTAZ H. A. K., ABDUL Y. A. F. (2019). The field-dependent rheological properties of plate-like carbonyl iron particle-based magnetorheological elastomers. In: *Results in Physics,* Vol. 12, No., pp. 2146–2154.

[6] ZHANG, G., WANG, H., WANG, J., JIAJIA Z., QING, O. (2019). Dynamic rheological

properties of polyurethane based magnetorheological gels studied using oscillation shear tests. In: *RSC Adv,* Vol. 9, No.18, pp. 10124-10134.

[7] NAM, T. H., PETRÍKOVA, I., MARVALOVA, B. (2020). Experimental characterization and viscoelastic modeling of isotropic and anisotropic magnetorheological elastomers. In: *Polymer Testing,* Vol. 81, No., pp. 1062-1072.

[8] VATANDOOST, H., HEMMATIAN, M., SEDAGHATI, R.,SUBHASH, R. (2020). Dynamic Characterization of Isotropic and Anisotropic Magnetorheological Elastomers in the Oscillatory Squeeze Mode Superimposed on Large Static Pre-strain. In: *Composites Part B: Engineering,* Vol. 182, No., 107648.

[9] AGIRRE-OLABIDE, I., ELEJABARRIETA, M. J. (2018). A new magneto-dynamic compression technique for magnetorheological elastomers at high frequencies. In: *Polymer Testing,* Vol. 66, pp. 114-121.

[10] MICHAL, M., S., PETR, L., PETR E., HIEP, L., C., VLADIMÍR, K., LE V., S., LUKÁŠ, V., ELIF, B., TOTKA B. (2018). Evaluation of Mechanical Properties of Composite Geopolymer Blocks Reinforced with Basalt Fibres. In: *Manufacturing Technology,* Vol. 18, No.5, pp. 861-865.

[11] BODNARUK, A. V., BRUNHUBER, A., KALITA, V. M., MYKOLA, M. K., PETER, K., ANDREI, A. S., ALBERT, F. L., SERGEY, M. R., MIKHAIL, S. (2019). Magnetic anisotropy in magnetoactive elastomers, enabled by matrix elasticity. In: *Polymer,* Vol. 16, No., pp. 63-72.

[12] AGIRRE-OLABIDE, I., KUZHIR, P., ELEJABARRIETA, M. J. (2018). Linear magneto-viscoelastic model based on magnetic permeability components for anisotropic magnetorheological elastomers. In: *J. Magn. Magn. Mater,* Vol. 446, pp. 155–161.

[13] ZUZANA, G., PAVOL, Š., ALENA, B. (2020). Microstructure and Selected Properties of Si3N4+SiC Composite. *Manufacturing Technology*, Vol. 20, No.3, pp. 293-299.

[14] DRAHOMÍR G., JIŘÍ K., DALIBOR, H. (2019). Magnesium Composite Materials Prepared by Extrusion of Chemically Treated Powders, In: *Manufacturing Technology*, Vol. 19, No.5, pp. 740-744.

[15] NEDJAR, A., AGUIB, S., DJEDID, T., NOUR, A., MELOUSSI, M. (2019). Measurements and identification of smart magnetomechanical elastomer composite materials properties in shear mode. In: *Materials Research Express,* Vol. 6, No., 085707

[16] SUN, S. S., YANG, J., LI, W. H., DU, H., ALICI, G., YAN, T.H., MASAMI, N. (2017). Development of an isolator working with magnetorheological elastomers and fluids. In: *Mechanical Systems and Signal Processing,* Vol. 83, pp. 371-384.

Appendix A: Supplementary data (Experimental results obtained by the Dynamic Mechanical Analyzer, Metravib DMA +450).

Tab. 2 *Experimental results B=0mT, f=50Hz, β=0°*

Test 1			
Shear strain	G'(Pa)	G"(Pa)	Loss factor
0.00192032	1832829.120	432364.5888	0.235900109
0.00484875	1284667.776	314776.2816	0.245025436
0.00973429	1016428.992	249581.6448	0.24547546
0.01952960	818620.2240	220044.8448	0.268799668
0.04856240	680515.9680	189552.7488	0.278542691
0.07134710	619680.5760	152053.9584	0.279374737
Test 2			
Shear strain	G'(Pa)	G"(Pa)	Loss factor
0.00192978	2832015.168	549072.5952	0.193880528
0.00493925	1985253.888	406397.2032	0.204707925
0.00720365	1748054.784	365511.1296	0.209095924
0.00971442	1553543.424	323908.4352	0.209496544
0.01944100	1218576.768	245279.5392	0.210836170
0.03358440	1004655.936	210453.1968	0.210877881

Test 3			
Shear strain	G'(Pa)	G"(Pa)	Loss factor
0.00191313	2069224.704	381353.5680	0.184297804
0.00481564	1580559.552	341745.3888	0.216217977
0.00719273	1414183.296	314726.2848	0.222549853
0.00955027	1313320.704	294794.2272	0.224464768
0.01925760	1083264.000	243741.5424	0.225006593
0.03359460	947385.7920	216768.8640	0.228807383
Test 4			
Shear strain	G'(Pa)	G"(Pa)	Loss factor
0.00192473	3310508.352	758213.3760	0.229032310
0.00482650	2301793.152	567130.3680	0.246386330
0.00721707	1973397.504	501022.0992	0.253888078
0.00965702	1757131.584	458754.5664	0.261081510
0.01945030	1406892.096	358151.4816	0.264569261
0.03414850	1198197.120	292599.7248	0.264699990
Test 5			
Shear strain	G'(Pa)	G"(Pa)	Loss factor
0.00192086	2287371.456	446022.6432	0.194993534
0.00479570	1699159.104	370837.5744	0.218247705
0.00730173	1493618.688	332541.8112	0.222641705
0.00976254	1374769.152	305944.7040	0.226542602
0.01953220	1130903.808	248726.3424	0.229935896
0.03426130	980883.6480	219001.4592	0.230269559

Tab. 3 *Experimental results B=150mT, f=50Hz, β=0°*

Test 1			
Shear strain	G'(Pa)	G"(Pa)	Loss factor
0.00482521	2146130.496	703627.584	0.327858714
0.00967595	1540270.464	540896.3328	0.351169710
0.01934670	1213273.536	401948.6784	0.353292711
0.04831200	871581.1200	297939.264	0.353837675
0.07339940	765784.3200	276772.1664	0.361423131
0.09605940	714287.6160	231708.384	0.362390874
Test 2			
Shear strain	G'(Pa)	G"(Pa)	Loss factor
0.00479868	2877089.664	739541.9520	0.257045153
0.00720446	2453348.928	638268.6720	0.260162207
0.00953910	2190163.392	576791.0592	0.263355264
0.01930420	1670863.296	448799.8464	0.268603570
0.03348680	1409457.408	366462.2592	0.270002365
0.04774690	1275156.480	327426.6624	0.271773712
Test 3			
Shear strain	G'(Pa)	G"(Pa)	Loss factor
0.00482997	2482323.264	698193.4080	0.281266110
0.00724993	2150933.760	612395.3280	0.288711384
0.00966975	1943827.968	555301.9584	0.291674436
0.01936920	1540413.312	429654.0480	0.293921277
0.03382170	1294958.784	347533.1136	0.293933880
0.04869460	1151706.048	307070.2272	0.293992050

Tab. 4 *Experimental results B=250mT, f=50Hz, β=0°*

Test 1			
Shear strain	G'(Pa)	G"(Pa)	Loss factor
0.00481840	3152750.592	1033410.048	0.327780463
0.00976011	2182366.272	734054.2080	0.346357016
0.01911990	1626211.392	532352.2368	0.347357341
0.04810510	1126213.632	348187.2384	0.349166244
0.07312640	890823.9360	294706.1376	0.351824224
0.09675360	754648.1280	320599.7184	0.352833385
Test 2			
Shear strain	G'(Pa)	G"(Pa)	Loss factor
0.00488696	2692910.976	757058.6880	0.281130232
0.00723629	2348825.856	667522.7520	0.294194228
0.00967814	2128935.168	605651.7120	0.304485747
0.01926820	1690617.984	477558.1248	0.304675479
0.03405320	1421575.680	389343.5328	0.311881678
0.04877340	1280673.984	346123.0848	0.314896351
Test 3			
Shear strain	G'(Pa)	G"(Pa)	Loss factor
0.00479046	2929318.464	818263.1040	0.279335659
0.00720768	2498744.832	704681.0880	0.292014025
0.00962822	2248617.984	630703.6800	0.295485029
0.01936040	1753304.448	481754.2848	0.299769328
0.03395110	1463614.656	388234.0800	0.301257032
0.04867800	1316897.856	344818.4064	0.302841421

Tab. 5 *Experimental results B=325mT, f=50Hz, β=0°*

Test 1			
Shear strain	G'(Pa)	G"(Pa)	Loss factor
0.00475383	2965982.784	724816.7040	0.244376572
0.00726697	2580620.544	633542.7840	0.255500171
0.00969859	2313459.072	576327.3984	0.259119341
0.01908080	1703498.112	463652.4672	0.262176684
0.03362950	1316022.912	359488.8960	0.263163098
0.04755610	1123957.824	313615.6416	0.264279450
Test 2			
Shear strain	G'(Pa)	G"(Pa)	Loss factor
0.00484973	2539045.824	724108.4160	0.285189188
0.00722532	2187401.664	644988.4800	0.298865132
0.00964776	1976379.456	587461.8048	0.302541404
0.01925050	1524289.344	461406.1824	0.302552492
0.03366910	1238361.216	369090.0672	0.302577179
0.04797320	1083871.104	326624.9280	0.302580342
Test 3			
Shear strain	G'(Pa)	G"(Pa)	Loss factor
0.00483404	2917610.880	736339.7760	0.252377649
0.00726212	2526391.872	653690.3040	0.262744620
0.00969288	2294115.072	594897.6384	0.265314646
0.01931790	1816645.632	468517.6320	0.266902600
0.03391860	1511861.568	384718.2336	0.267065740
0.04878650	1346509.056	344926.1376	0.267103251